THE JOURNAL OF PHYSICAL CHEMISTRY C

Article

pubs.acs.org/JPCC

Infrared Study of (Poly)tungstate Ions in Solution and Sorbed into Layered Double Hydroxides: Vibrational Calculations and In Situ Analysis

A. Davantès, D. Costa, and G. Lefèvre*

Institut de Recherche de Chimie Paris, CNRS−Chimie ParisTech, 11 rue Pierre et Marie Curie, 75005 Paris, France

Supporting Information

ABSTRACT: In situ attenuated total reflection infrared spectroscopy (ATR-FTIR) was used to study the speciation of (poly)tungstate ions in solution and the sorption process into layered double hydroxides (LDHs). In the first section, the W(VI) speciation in solution was performed by comparison of thermodynamical calculations and infrared spectroscopy of solutions as a function of pH. Then, the exchange mechanism within LDHs was followed in real time with the in situ ATR technique and compared with batch experiments characterized by powder X-ray diffraction (PXRD), elemental analysis, and FTIR. Decomposition of the (W−O) stretching vibration bands, between 800 and 1000 cm^{-1}, has allowed the identification of the high affinity of LDHs for the polytungstate species, $W_7O_{24}^{6-}$, despite the presence of carbonate ions and higher charged polytungstate ions in solution. This was confirmed by the DFT methods used to investigate the structure and the vibrational modes of this anion, and very good agreement with experimental spectra has been obtained. The affinity series $W_7O_{24}^{6-} > CO_3^{2-} > WO_4^{2-} > SO_4^{2-}$ has been directly deduced from those results.

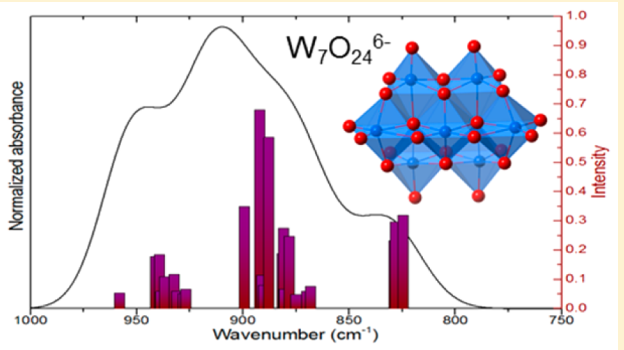

1. INTRODUCTION

Layered double hydroxides (LDHs), or hydrotalcite-like compounds, are anionic clays formed by brucite-type layer $M(OH)_2$ in which M^{3+} are partially substituted with M^{2+} leading to a net positive charge on the metal hydroxide layer. The excess positive charge is balanced with interlayer exchangeable anions.[1−3] A broad variety of anions can be introduced in the interlayer (halides, organic species, oxoanions, and so on) along with some water molecules. This has resulted in increasing interest in these materials for various applications like catalysis, medicals, anion exchangers, electrode materials, and so on.[4−10] Given that they are easily synthesized by cheap methods and have high anion exchange capacities, many studies have focused on decontamination capacity of the LDHs because they are good candidates for wastewater treatment to scavenge pollutants present as oxyanions (selenate, arsenate, molybdate, vanadate, and so on).[11−17]

(Poly)tungstate species are used in several fields such as catalysis and medicine.[18−23] However, research on tungsten toxicity is in its infancy,[24] and its environmental consequences has not been investigated in detail. Clausen et al.[25] found that firing range soils are highly contaminated with tungsten and that, in general, tungstate and (poly)tungstate species are weakly retained, a fact attested to by the high mobility of those species in groundwater. W(VI) speciation in solution is complicated due to the formation of many polyanions like the paratungstate A ($W_7O_{24}^{6-}$).[26,27] Tungstate can also form polyoxometalate species (POMs) in solution with one or two other metal atoms with similar structure.[28,29] Many studies have been carried out on sorption of POMs into layered double hydroxides,[30−34] but very few directly with tungstate species.[35−39] In those studies, the characterization of sorbed W(VI) was performed ex situ on dried solids after the sorption using several methods: by X-ray diffraction technique to measure the interlayer distance and determine the size of the intercalated anions, by elemental analysis, and by spectroscopic methods such as Raman or infrared with the KBr pellet technique. To the best of our knowledge, (poly)tungstate species in solution and sorbed into LDH have never been followed by in situ infrared spectroscopy.

The objectives of this present study are the identification of the exchange mechanisms and the speciation of sorbed species into LDHs. To characterize W(VI) species in solution and during the exchange in LDH, we have used in situ attenuated total reflection (ATR) infrared spectroscopy. As previously demonstrated for Mo(VI),[40] this method allows for the monitoring of ion in the hydrolyzed state or during the ion exchange processes, leading to structural information about those species for different concentrations and pH values. As the polymerization occurs at low pH, a LDH present in mining region with good stability at low pH was chosen,[41] with a ZnAl-

Received: February 16, 2015
Revised: April 13, 2015
Published: May 13, 2015

DOI: 10.1021/acs.jpcc.5b01578
J. Phys. Chem. C 2015, 119, 12356−12364

(SO_4,CO_3) composition. This solid presents two different exchangeable anions that absorb in mid-IR, which is useful to follow the exchange mechanism with (poly)tungstate ions. Furthermore, a density functional theory (DFT) study upon the paratungstate A has been done to help determine the speciation of the sorbed species into the LDH interlayer. W polyoxometalates, especially with Keggin structure, have already been successfully modeled using DFT studies.[42−49] In particular, Alizadeh and Salimi[48] have carried out with DFT (B3LYP) vibration frequencies calculations of Anderson type W polyoxometalates that successfully compared to experiment.

2. MATERIALS AND METHODS

2.1. Materials. All solutions and suspensions in aqueous phase were prepared using purified water (Milli-Q, Millipore) with a resistivity of 18.2 MΩ·cm. An aqueous tungstate solution (0.1 M) was prepared from $Na_2WO_4{\cdot}2H_2O$ (Acros Organic), and metatungstate solution came from $Na_6O_{39}W_{12}{\cdot}H_2O$ (Alfa Aesar). Acidification was performed with a 0.1 M HCl solution (Prolabo).

Samples of Zn−Al sulfate carbonate LDHs with a $[Zn^{2+}]/[Al^{3+}]$ ratio equal to 3/1 (general formula $[Zn_{0.73}Al_{0.27}(OH)_2]$-$(SO_4,CO_3)_{0.14}{\cdot}mH_2O$), were provided by C. Ardau (Univ. Cagliari) and were described in previous articles.[40,41] The provided LDH particles present a sand-rose shape with a size about 1 μm determined with scanning electron microscopy (SEM).

2.2. Batch Experiments. Batch adsorption experiments were carried out with sodium tungstate and metatungstate solution. Approximately 50 mg of LDH was suspended in beakers with 30 mL of aqueous tungstate solution at 10^{-2} M or metatungstate solution at 10^{-3} M. The suspensions were left for 1 day or 1 week under vigorous stirring with a fixed pH of 5.50 with HCl. For one batch experiment, the tungstate solution was aged for 1 week before sorption during 1 day. Solids were collected by centrifugation, washed with Milli-Q water, and dried in a desiccator under a dry atmosphere.

The collected solid materials were analyzed by XRD and by infrared spectroscopy both before and after sorption experiments. Powder X-ray diffraction (PXRD) patterns were obtained on a PANalytical X'Pert PRO diffractometer operating at 40 kV and 45 mA with a step size 0.039 2θ deg, and step scan 148 s using Cu Kα radiation (λ = 1.54050 Å) and a PIXcel detector. Fractions of the solids were dissolved in 10% v/v HCl (12 M), filtered at 0.45 μm, and analyzed by inductively coupled plasma atomic emission spectrometry (ICP-AES) for the analysis of W, S, Na, Zn, and Al. Infrared spectra of solids were recorded with the ATR accessory described subsequently.

2.3. In Situ ATR-IR Spectroscopy. The experimental conditions and setup are similar to those described in our previous article.[40] The ATR-FTIR spectra were collected with a dry-air-purged Thermo Scientific Nicolet 6700 FT-IR equipped with a MCT detector. Spectral resolution was 4 cm^{-1} and spectra were averaged from 256 scans. The horizontal ZnSe crystal with a single reflection (A = 2.54 mm^2) and an angle of incidence of 45° (Smart PIKE) was coated with 1 μL of the LDH suspension (1 g/L) which was dried under a flow of N_2 (procedure repeated three times). The flow cell was placed on the ATR accessory and a background recorded when the solution (degassed water without tungstate ions) reached the LDH film for conditioning, with a constant flow rate of 1 mL/min using a peristaltic pump (Ismatec S.A.) at room temperature. All experimental solutions were kept under a continuous stream of nitrogen in order to avoid the LDH contamination with carbonate ions. After stabilizing for at least 30 min, a background spectrum was recorded and a given volume of a 0.1 M sodium tungstate solution stock was subsequently added to the circulating solution. Anion exchange into the layered double hydroxides was followed by the acquisition of spectra in minute steps. When the intensity did not vary more than 5% between two successive spectra, equilibrium is assumed to be reached. The pH was adjusted with HCl using a pH meter and an automatic titrator (Metrohm with Tiamo software). For data reprocessing OMNIC software was used and spectra were decomposed with Gaussians peaks and linear baseline made by interpolation using OriginPro 8.6 software. The fitting procedure was performed until a value of 0.999 was obtained for the coefficient R^2, and the decomposition achieved with the minimum number of peaks with different areas, wavenumbers, and widths to fit the spectra.

2.4. Computational Methods. The calculations have been performed using an ab initio plane-wave pseudopotential approach as implemented in VASP.[50,51] The Perdew−Burke−Ernzerhof (PBE) functional was chosen to perform the periodic DFT calculations.[52,53] The valence electrons are treated explicitly, and their interactions with the ionic cores are described by the projector augmented-wave method (PAW),[54,55] which allows the use of a low energy cutoff equal to 400 eV for the plane-wave basis. The integration over the first Brillouin zone is performed using the Γ-point.

Calculations were performed on the bulk $K_6[W_7O_{24}]{\cdot}4H_2O$ from the structure of Evans,[56] as it is known that the paratungstate A is isostructural to the heptamolybdate anion.[26,27,57,58] First, the proton positions were relaxed. Then both atom positions and cell size and volume were relaxed. The obtained anion geometry is shown and analyzed in the Supporting Information. The harmonic frequencies were calculated after determination of the Hessian matrix. Vibration intensities were evaluated through linear response calculations. This gives the matrix of Born effective charges (BEC), which refers to change of atoms' polarizabilities with respect to an external electric field. The BEC tensor is a key to calculate the vibrational intensities, using the formula by Gianozzi and Baroni.[59−63]

3. RESULTS AND DISCUSSION

3.1. (Poly)tungstate in Solution. ATR-FTIR spectra of W(VI) species in aqueous solution, with 1.0 M NaCl, from pH 9.65 to 5.12 are presented in Figure 1. The speciation of W(VI) in aqueous solution has been studied, but the investigation remains difficult because of the slow reactions which occur upon acidification and the formation of kinetic intermediate species.[26,27,64] Acidification of a sodium tungstate solution leads to the formation of different polyoxoanion according to the following equation:

$$p[WO_4^{2-}] + qH^+ \leftrightarrows [(WO_4)_pH_q]^{(2p-q)-} \quad (1)$$

The speciation diagram of W(VI) with a concentration of 0.1 M is presented in Figure 2 and was calculated from thermodynamic data by Cruywagen et al.[26,27] The major species in solution at a pH > 7.8 are tungstate ions WO_4^{2-} (>99%). The first two spectra, recorded at pH 9.65 and 7.96 respectively (Figure 1), are identical with a single band at 827 cm^{-1} and can be attributed to the asymmetric stretching

DOI: 10.1021/acs.jpcc.5b01578
J. Phys. Chem. C 2015, 119, 12356−12364

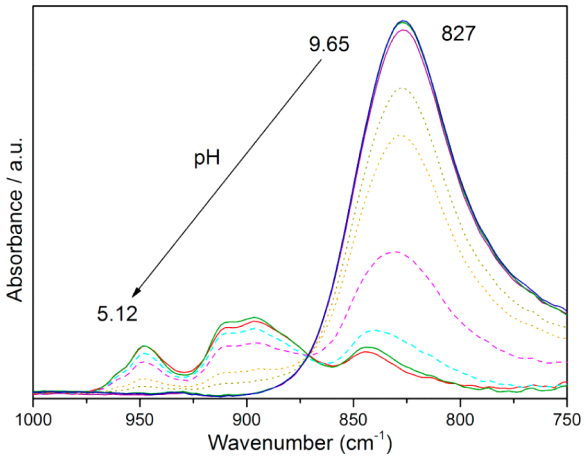

Figure 1. ATR-IR spectra of W(VI) (0.1 M) in aqueous solution (1.0 M NaCl) at various pH values: 9.65, 7.96, 7.65, 7.43, 6.99, 6.49, 5.97, 5.12 from the top to the bottom.

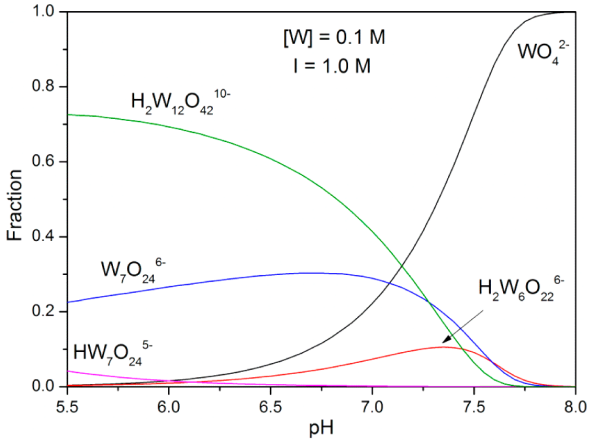

Figure 2. Speciation diagram of W(VI) at 0.1 M (calcultated from Cruywagen et al.[26,27]).

vibrational mode ν_3 of the free tetrahedral WO_4^{2-} anion with T_d symmetry.[65] The symmetric stretching vibration ν_1 visible in Raman spectroscopy at 931 cm^{-1} is not detected in the infrared spectra.

Polytungstate species are formed from pH 7.80 and became the major species in solution below pH 7.15. The two more stable, and formed first, polyanions are the paratungstate A and B (respectively $W_7O_{24}^{6-}$ and $H_2W_{12}O_{42}^{10-}$), which coexist between pH 8 and 5. Paratungstate A ions have a C_{2v} symmetry, and the structure is shown in Figure 3, while paratungstate B anions have a lower symmetry C_1 and a larger structure (Figure 3) according to the crystallographic parameter of Allmann.[66] Tungsten atoms have a distorted octahedral coordination

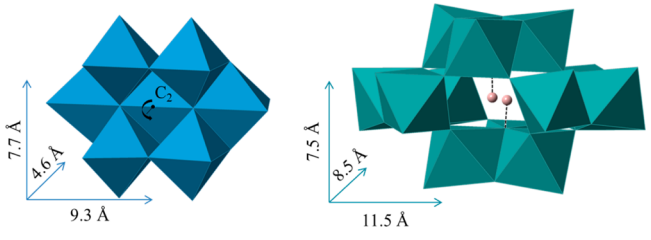

Figure 3. Structure of polyoxoanions $W_7O_{24}^{6-}$ and $H_2W_{12}O_{42}^{10-}$.

structure (WO_6). At a lower pH, different metatungstate ions are created with slow kinetic, the most stable of which are α-metatungstate ions with Keggin structure ($H_2W_{12}O_{40}^{6-}$).[26]

There is a significant change in spectra when polytungstate species appear in solution below pH 7.65 (Figure 1). The band at 827 cm^{-1} decreases with the concentration of tungstate ions (WO_4^{2-}) in solution, while several new overlapping peaks appear between 860 and 970 cm^{-1}: 897, 911, 948 cm^{-1} with a slight shoulder at 962 cm^{-1}. However, the two paratungstate ions in solution cannot be distinguished from those spectra. Indeed, the recorded spectra are composed of both species, and according to the speciation diagram (Figure 2), the paratungstate A is always a minor species between pH 5 and 8. Thus, the spectrum of $W_7O_{24}^{6-}$ species, which is suspected to be sorbed in LDH, cannot be extracted from the solution spectra.

3.2. Characterization of Batch Experiments. A preliminary study of the (poly)tungstate sorption upon layered double hydroxides was performed with batch experiments followed by routine analyses to characterize the LDH interlayer and sorbed ions, using powder X-ray diffraction (XRD), elemental analysis (ICP-OES), and spectroscopic technique (FTIR).

Figure 4 shows the XRD patterns of layered double hydroxide before (a) and after the tungstate sorption in batch

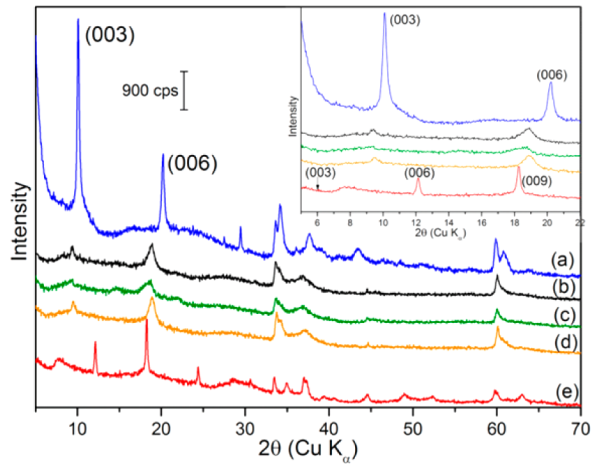

Figure 4. X-ray diffraction patterns of (a) LDH-(SO_4,CO_3), (b) LDH-W 1 day, (c) LDH-W 1 week, (d) LDH-W 1 day with an aged tungstate solution, (e) LDH-W_{12}. See text for details about the experimental protocols of preparation.

with different experimental conditions (b–e). Knowing that the anion exchange capacity (AEC) of the solid is 2.05 $mol \cdot kg^{-1}$, the minimum amount of tungstate ions in solution for the saturation of the LDH can be calculated. To saturate the LDH, a concentration of 10^{-2} M of sodium tungstate was chosen and 10^{-3} M for the metatungstate solution, in order to have approximately the same tungsten amount in every batch experiment. The pH of 5.50 is the best possible selection, due to the compromise between LDH stability in solution and the state of polymerization from the speciation diagram (Figure 2).

The XRD patterns of initial LDH (Figure 4a) show a clear layered structure with a d_{003} spacing of 8.75 Å (2θ = 10.1°) corresponding to the distance between the adjacent hydroxide layers. Patterns of LDH sorbed in batch experiment are presented in Figure 4b–e according to their experimental conditions: LDH sorbed with sodium tungstate at pH 5.50 and 10^{-2} M during 1 day (b), 1 week (c), with an aged tungstate

DOI: 10.1021/acs.jpcc.5b01578
J. Phys. Chem. C 2015, 119, 12356–12364

Table 1. Chemical Composition of LDH before and after Sorption Experiments

sample	chemical composition (mmol/g) Zn	Al	DiAn[a]	W	molar ratio Zn:Al	empirical formula
LDH-SO_4,CO_3	6.51	2.4	1.2	0	2.72	$[Zn_{0.73}Al_{0.27}(OH)_2](SO_4,CO_3)_{0.14}\cdot mH_2O$
LDH-W 1 day	4.08	1.63	0.21	1.41	2.50	$[Zn_{0.71}Al_{0.29}(OH)_2](SO_4,CO_3)_{0.04}(W_7O_{24})_{0.247}\cdot mH_2O$
LDH-W 1 week	3.87	1.57	0.12	1.56	2.47	$[Zn_{0.71}Al_{0.29}(OH)_2](SO_4,CO_3)_{0.02}(W_7O_{24})_{0.286}\cdot mH_2O$
LDH-W aged[b]	4.53	1.79	0.31	1.35	2.54	$[Zn_{0.72}Al_{0.28}(OH)_2](SO_4,CO_3)_{0.05}(W_7O_{24})_{0.214}\cdot mH_2O$
LDH-W_{12}	4.22	1.62	0	3.26	2.61	$[Zn_{0.72}Al_{0.28}(OH)_2](H_2W_{12}O_{40})_{0.047}\cdot mH_2O$

[a]Dianion (sulfate and carbonate) concentration to balance positive excess charge of Al^{3+} vs Zn^{2+}. [b]1-day equilibration with an aged tungstate solution.

solution prepared 1 week before the sorption (d), and sorbed with metatungstate solution at the same pH and 10^{-3} M during 1 day (e). The sorption patterns present broader peaks that can be explained by structural disorder like low crystallinity, interstratification, stacking disorder, and turbostraticity.[67] The relative basal reflections intensities (00*l*) of the solids after sorption are reversed compared to the original one, and even the (003) harmonic in the metatungstate sorption is too low to be detected. According to Thomas et al.,[68] these intensities are sensitive to the interlayer content, such as the nature of the intercalate species and the concentration of the intercalate species (W) which depend on the Zn/Al ratio while the water content is dependent on the drying conditions and atmospheric humidity.

In all samples of LDH sorbed with W(VI), a shift of the 003 and 006 reflections to lower angles was observed, suggesting a complete exchange with the tungstate species, correlated with a larger interlayer distance. With Na_2WO_4 (Figure 4b–d), a basal spacing of 9.40 Å was found for the three experimental conditions: from fresh solutions prepared at pH 5.50, or from a solution aged at pH 5.50. Subtracting the size of the layer (4.8 Å)[69] from 9.4 Å, a space of 4.6 Å remains between the two layers of the LDHs. Del Arco et al.[36,37] observed a decrease of the interlayer distance depending on the contact times with the solution during the exchange, resulting from different orientation and interactions between the anion and the brucite-like layers. They have suggested that such a small distance can be attributed to the paratungstate A ($W_7O_{24}^{6-}$), with its C_2 axis perpendicular to the layers without its hydration shell and thus directly in contact with the layer structure. This geometry is possible by the shifting of the hydroxyl groups with the oxygen atoms of the polytungstate anion, or, with an option suggested by Wang et al.[70] for different POM pillared LDHs, defects in the layer created during the sorption reaction by the removal of some OH groups along with the divalent metal ions. Thus, the sorption mechanism can consist of two steps: first the exchange between the interlayer anion (in our case carbonate and sulfate ions) with paratungstate anions, then a change of the anion orientation and a loss of the hydratation shell in several hours, leading to a strong interaction between the polyanions and the layered surface.

According to the speciation of the polytungstate ions, calculated by Cruywagen et al.,[26,27] at pH 5.5, two major species are present in solution: $W_7O_{24}^{6-}$ and $H_2W_{12}O_{42}^{10-}$, the paratungstate A and B ions, respectively. As mentioned previously, the comparison of their structure presented in Figure 3 shows that the paratungstate B is larger than the paratungstate A, with a smallest length of 7.5 Å while the smallest length of the paratungstate A is 4.6 Å. In order to understand the behavior of the layered double hydroxide with a large species like the paratungstate B, batch experiment with metatungstate ions were performed (Figure 4e). The structure of the paratungstate B can be found in in various solid compounds, but its solubility is too low to use in solution.[26] To overcome this problem we used the metatungstate ion ($H_2W_{12}O_{40}^{6-}$), which has a similar structure and size as the paratungstate B and is thermodynamically stable in solution, which ensures that it is the only ion in solution. According to previous studies,[35,31−33,71] all diffraction peaks in pattern of this latter experiment can be attributed to a LDH-$H_2W_{12}O_{40}^{6-}$. The difficulty created by the weak harmonic peak (003) has been overcome by using d_{006} = 7.28 Å (2θ = 12.13°) to calculate the basal spacing of 14.5 Å which corresponds to the results obtained for this sorbed species in previous studies. According to those results, the only anion which can fit with a space of 4.6 Å, from the Na_2WO_4 solution, is the paratungstate A: $W_7O_{24}^{6-}$ ions.

The elemental chemical analysis is another method that can be used to determine the speciation of W(VI) ions in LDH. The excess positive charge of the layer induced by Al^{3+} is balanced with the interlayer anion $[(WO_4)_pH_q]^{(2p-q)-}$. Results of the chemical analysis are presented in Table 1. Both carbonate and sulfate ions are present in the LDH we used, and the total concentration has been calculated (DiAn), because carbonate cannot be measured by chemical analysis using ICP-OES. The Zn/Al ratio is about 2.5 for the three sorption experiments with Na_2WO_4 and at 2.61 with metatungstate ions, which is less than the 2.72 of the original LDH. This can be explained by a small dissolution of Zn^{2+} at pH 5.5 leading to a decrease of the Zn/Al ratio.

Sulfate and carbonate ions are totally exchanged with metatungstate ions (LDH-W_{12}) only even though the remaining amount is very low in the other LDHs. According to the chemical composition, the exchange with metatungstate ions is confirmed but the identification of the interlayer ions for the sorption of Na_2WO_4 is challenging. According to tungstate amounts, both paratungstate A and B can be present inside the LDH interlayer and compensate the excess positive charge. However, the XRD results have shown that the basal spacing is too small for the paratungstate B ions, and thus paratungstate A ions ($W_7O_{24}^{6-}$) are most likely the interlayer ions leading to the empirical formula presented in Table 1.

Batch samples of layered double hydroxides sorbed with metatungstate and polytungstate were analyzed after drying with ATR-FTIR spectroscopy (Figure 5). A band at 1106 cm^{-1} corresponding to the ν_3 of internal SO_4^{2-} anions confirms that the exchange is not complete with the LDH sorbed with polytungstate. For metatungstate ions, this band is not visible, which confirms the total exchange. Between 1000 and 700 cm^{-1}, spectra present different bands corresponding to the tungstate species in the layered double hydroxide. Free metatungstate ions in solution (spectrum not show) present

DOI: 10.1021/acs.jpcc.5b01578
J. Phys. Chem. C 2015, 119, 12356−12364

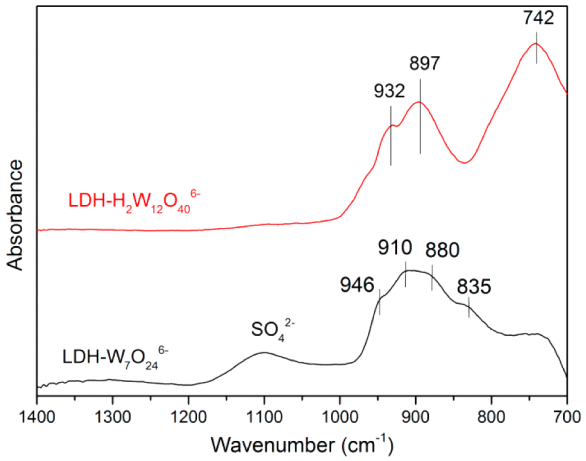

Figure 5. ATR-FTIR spectra of LDH powders after sorption of metatungstate and polytungstate ions in batch experiments.

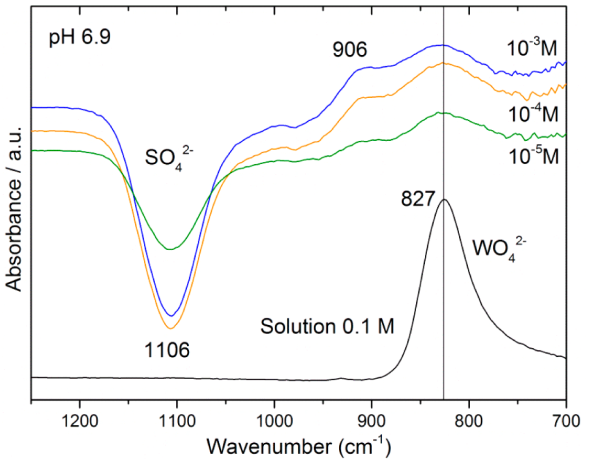

Figure 6. Spectra of tungstate ions exchanged into LDH for several concentrations, 10^{-5}, 10^{-4}, and 10^{-3} M, at pH 6.90 and comparison with the spectrum of free tungstate ions in aqueous solution (0.1 M).

the same band as the sorbed species into LDH (red), thus the sorption of $H_2W_{12}O_{40}^{6-}$ is confirmed. The spectrum of LDH sorbed with Na_2WO_4 solution presents a different band than metatungstate and is consistent with a heptatungstate ion.

However, the exchange mechanism takes place during the first hours of the experiment, which was not observed with those batch samples. In situ infrared spectroscopy allows the observation of the exchange mechanism directly in solution and with varying experimental conditions (pH, concentration) from the beginning of the exchange to equilibration state. Furthermore, the paratungstate A spectrum in solution is unknown and so further DFT study of this complex is required to confirm the band attribution and identify the various vibrations that occur in the complex.

3.3. In Situ Study of (Poly)tungstate Sorption in LDH.

First, we have studied the impact of the W(VI) concentration on LDH at a pH where no polymerization is expected for those concentrations using thermodynamical data, pH 6.90. The LDH we used presented two exchangeable interlayer species observable in infrared spectroscopy: sulfate and carbonate ions. To view that exchange, the background is set directly on LDH in the presence of water, thus all released species will be characterized by negative peaks, while sorbed species will lead to positive peaks. The ATR-IR spectra of tungstate ions upon sorption into layered double hydroxides for several concentrations at pH 6.90 are shown in Figure 6. The spectrum of free tungstate ions (WO_4^{2-}) in aqueous solution, obtained from 0.1 M $Na_2WO_4{\cdot}2H_2O$ stock solution, is also presented for comparison. Spectra of WO_4^{2-} sorbed into layered double hydroxides were recorded from an initial tungstate concentration of 10^{-5} M, equilibria were reached between 15 and 20 min after the addition of tungstate, and the pH was set to 6.90.

The band located at 1106 cm^{-1} is assigned to the triply degenerate asymmetric stretching vibration (ν_3) of the SO_4^{2-} anions, with T_d symmetry, in the LDH interlayer, and the band at 827 cm^{-1} characterizes the tungstate ions in solution. The exchange is extremely efficient, and a concentration of 10^{-4} M of W(VI) is enough to exchange more than 90% of the sulfate ions from the interlayer (obtained by the difference of the LDH spectra before and after exchange). Sorption spectra presented a positive band between 700 and 950 cm^{-1} corresponding to the sorption of tungstate ions into the LDH. This band is composed of a broad peak at 827 cm^{-1} and a shoulder at 906 cm^{-1} whereas the solution spectra consist of only one peak at 827 cm^{-1}. Therefore, there is a change of symmetry or structure of tungstate ions during the adsorption (inner-sphere complexes) or the polymerization of ions since LDH particles present a sand-rose morphology with a sufficiently small size (about 1 μm) to allow the observation of anion adsorption into LDH by ATR spectroscopy. To answer that question, the same experiment was made at a pH range between 10.50 and 7.50 with a LDH containing only carbonate ions (spectra not show). At those conditions, ionic exchange cannot take place because tungstate ions (WO_4^{2-}) cannot desorb carbonate from the interlayer (see results presented in Figure 7). Obtained spectra

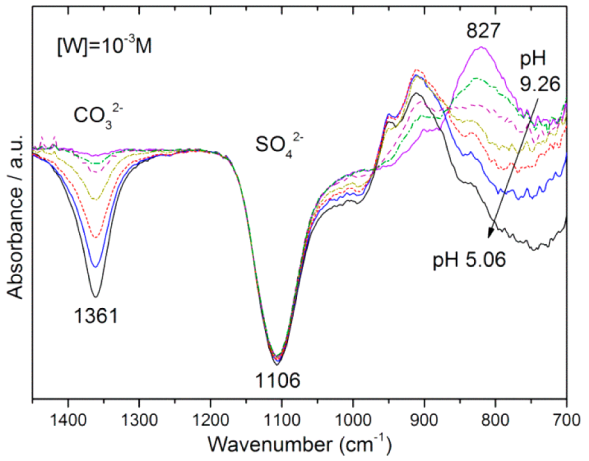

Figure 7. ATR-IR spectra of tungstate ions exchange into LDH at 10^{-3} M for decreasing pH values: 9.26, 8.07, 6.15, 5.68, 5.33, and 5.06 (from the top to the bottom).

did not present any bands of sorbed tungstate species. Thus, there is no adsorption of tungstate ions on the LDH surface during the ion exchange experiment, or the adsorption is too low to be detected by IR spectroscopy. Consequentially there is likely the beginning of polymerization at pH 6.90, which induces a change of tungstate spectra into LDH compared to the solutions.

Next, the effect of the pH on tungstate sorption into LDH was studied. IR spectra of tungstate sorbed into the LDH interlayer as a function of the pH values of the flowing solution are presented in Figure 7. The concentration of tungstate ions

DOI: 10.1021/acs.jpcc.5b01578
J. Phys. Chem. C 2015, 119, 12356−12364

was fixed at 10^{-3} M with the aim of a total exchange with sulfate ions from the LDH. Below a pH of 8.07, the WO_4^{2-} band (827 cm^{-1}) starts to decrease and the shoulder at 906 cm^{-1} increases. At lower pH, new peaks appear between 850 and 1000 cm^{-1}, which can be interpreted as the polymerization of W(VI) species, and a peak at 1361 cm^{-1} decreases, which can be assigned to ν_3 of CO_3^{2-} ions from the LDH interlayer. Since desorption of this species was not observed without tungstate in the same pH range (data not shown), it can be concluded that the polymerization of tungstate ions leads to desorption of the carbonate ions initially present in the LDH. However, spectra of this polytungstate species do not fit with solution spectra (Figure 1) but are similar to those of batch experiment with Na_2WO_4 (Figure 5). Thus, the same speciation was found in both experiments, and the exchange mechanism determined using in situ methodology can be extrapolated to batch experiments.

For further investigation, the decomposition of polytungstate band sorbed into LDH at pH 5.06 has been performed (Figure 8). This spectrum can be decomposed with three peaks

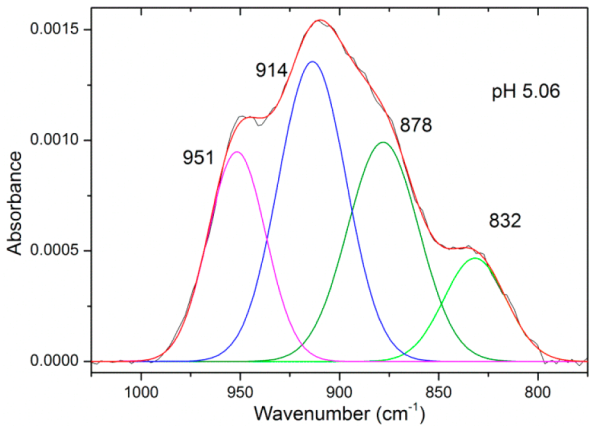

Figure 8. Decomposition of ATR-IR band of sorbed W(VI) at 10^{-3} M and pH 5.06 in four Gaussian peaks.

between 850 and 1000 cm^{-1} representative of the polymer species (878, 914, and 951 cm^{-1}) and one peak at 832 cm^{-1} which is probably a residue of the tetrahedral ions. In Table 2, the decomposition results along with data in the literature and sorption results of heptamolybdate ions in this LDH from our previous study are presented.[40] Del Arca et al.[36] worked on an Mg_2Al-LDH sorbed with the paratungstate A ions ($W_7O_{24}^{6-}$). Others have studied various tungsten polyoxometalate ions sorbed in different LDH including the paratungstate A.[38] George et al.[72] have recorded the IR spectrum of the paratungstate B, and Courcot and Bridgeman[58] have calculated the $W_7O_{24}^{6-}$ spectra in the gas phase. Attributions have been made according to Courcot and Bridgeman calculations, where $\nu_s(W{-}O_2)t$ and $\nu_{as}(W{-}O_2)t$ represent the symmetric and asymmetric vibration between tungsten atoms and terminal oxygen and $\nu(W{-}O{-}W)$ corresponds to all internal vibration of the structure.[58] Each system is in a different chemical environment, thus a shift of frequency between similar species is possible.

According to those results, the spectrum of paratungstate B anion does not match with our sorbed species. The $H_2W_{12}O_{42}^{10-}$ ion presents more peaks with a strong intensity for the bands around 850 cm^{-1}. The structure of $W_7O_{24}^{6-}$ ions is the same as the analogous molybdenum compound, the heptamolybdate ions ($Mo_7O_{24}^{6-}$), and this structure remains the same both in aqueous solution and in the solid state, respectively.[26,57,73] It appears that both spectra are similar for those species sorbed in our layered double hydroxide. There is a slight shift of 12−14 cm^{-1} between heptamolybdate bands and the polytungstate species sorbed in the LDH with the same intensity for each peak. Furthermore, our spectrum is in agreement with data in the literature confirming that the species sorbed into the LDH interlayer is the paratungstate A. Thus, it appears that there is a causal link between the ion size for the ions exchanged into the layered double hydroxide. Larger ions, relative to the size of the initial interlamellar space, will have difficulties in exchanging even if they have a very high charge compared to smaller and less charged ions.

3.4. DFT Study. Assuming that the structure of the paratungstate ions in solution is the same as in the solid state and with an analogous structure with the heptamolybdate, a density functional theory calculation was made to calculate the vibrational spectrum of tungstate species and confirm the experimental attribution.

The $W_7O_{24}^{6-}$ anion contains 31 atoms with a C_{2v} symmetry and has 87 normal modes leading to the irreducible representation:

$$\Gamma_{vib} = 26A_1(R, IR) + 18A_2(R) + 20B_1(R, IR) + 23B_2(R, IR)$$

The calculated vibrational frequencies compared with the cumulative curve obtained after decomposition of the

Table 2. Decomposition Results of ATR-IR Spectra during the Sorption into LDH of Polytungstate Species, at pH 5.06, of Batch Experiment of Metatungstate Ion Sorption and Comparison with Data in Literature[a]

sorption LDH-W	LDH-Mo [40]	LDH-W_7O_{24} [36]	LDH-W_7O_{24} [38]	$H_2W_{12}O_{42}^{10-}$ [72]	$W_7O_{24}^{6-}$ theoretical [58]	attribution
951 m	937 m	950	953	950 sh	928 w	$\nu_s(W{-}O_2)t$
914 s	902 s	925	922	936 s	915 m	$\nu_{as}(W{-}O_2)t$
					913 w	$\nu_s(W{-}O_2)t$
				890 sh	884 m	
					872 vw	
878 m	866 m	878	880	872 vs	866 vs	$\nu(W{-}O{-}W)$
					864 m	
				838 vs	844 s	
832 w	829 w		831		830 m	
				807 sh	821 m	

[a]Intensities: vs = very strong, s = strong, m = medium, w = weak, vw = very weak, sh = shoulder.

DOI: 10.1021/acs.jpcc.5b01578
J. Phys. Chem. C 2015, 119, 12356−12364

experimental spectrum at pH 5.06 of sorbed polytungstate at 10^{-3} M are presented in Figure 9. All vibrational frequencies are

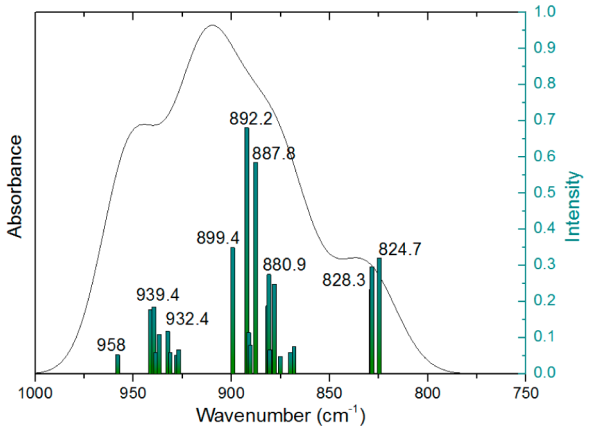

Figure 9. Infrared spectrum of LDH sorbed with polytungstate at 10^{-3} M and pH 5.06 compared with DFT calculated vibration frequencies of the $W_7O_{24}^{6-}$ anion.

listed in the Supporting Information (Table S1), and only frequencies between 960 and 820 cm^{-1} with intensity >1% are presented in Figure 9. The confrontation between theory and experiment demonstrates good agreement with only a small shift of approximately 10 cm^{-1} for the most intense peaks.

Representations of the principal vibration of the paratungstate A are presented in the Supporting Information (Figure S3). There are three characteristic vibration areas in the calculated spectrum. The first peak at 958 cm^{-1} is assigned to the symmetric stretching (ν_1) of the octahedral structure. Between 950 and 850 cm^{-1}, all peaks are due to asymmetric stretching vibrations of the octahedral structure with much internal coupling. The last block (between 850 and 800 cm^{-1}) corresponds to the asymmetric stretching vibration of the pseudoterminal oxygen atoms. Indeed, the paratungstate anion possesses two oxygen atoms bonded to two tungsten atoms (including the metal center), creating one long bond and one short bond. Due to this short bond being closer to the bond length of the tungsten−terminal oxygen bond (1.79 to 1.76 Å), they have been called pseudoterminal atoms.[58] These results suggest that the species sorbed into the layered double hydroxide at low pH in the present work is definitely the paratungstate A ions.

4. CONCLUSIONS

The investigation of (poly)tungstate sorption into layered double hydroxides was followed by in situ ATR-FTIR spectroscopy. This method allowed the following of the exchange mechanism directly inside the LDH and obtained information about the speciation of the sorbed species. The uptake of W(VI) within $[Zn_{0.73}Al_{0.27}(OH)_2](SO_4,CO_3)_{0.14}\cdot mH_2O$ LDH was followed by varying experimental conditions such as tungstate concentration and pH. The obtained spectra indicated that (poly)tungstate ions are electrostatically sorbed into the LDH interlayer with a preference for the paratungstate A anion ($W_7O_{24}^{6-}$). Thus, this species is isolated into the LDH and its infrared spectrum has been observed for the first time. The DFT calculation allowed us to confirm the attribution of this spectrum and its similarity with the heptamolybdate structure, and to identify the vibrations which occur in the polymer.

Furthermore, we highlighted a size effect for ion exchanged with layered double hydroxide. Indeed, the paratungstate A is a species with six charges while the paratungstate B has ten charges but the smaller species is preferentially sorbed. The affinity series $W_7O_{24}^{6-} > CO_3^{2-} > WO_4^{2-} > SO_4^{2-}$ was directly shown by the ATR-IR experiments and is similar to the one obtained with (poly)molybdate ions in our previous study,[40] which shows that both ions have the same behavior with Zn−Al-LDHs.

■ ASSOCIATED CONTENT

Supporting Information

The optimization of the W_7O_{24} anion is detailed and its structure and average W−O bond are presented in Figures S1 and S2. Calculated IR vibrational frequency and principal eigenvectors of paratungstate A ions are also presented in Table S1 and Figure S3. The Supporting Information is available free of charge on the ACS Publications website at DOI: 10.1021/acs.jpcc.5b01578.

■ AUTHOR INFORMATION

Corresponding Author

*E-mail: gregory.lefevre@chimie-paristech.fr.

Notes

The authors declare no competing financial interest.

■ ACKNOWLEDGMENTS

A.D. thanks University Pierre et Marie Curie (Paris) for financial support. We are indebted to Dr. Carla Ardau (Department of Chemical and Geological Sciences, University of Cagliari, Italy) for the preparation of the layered double hydroxide.

■ REFERENCES

(1) Forano, C.; Hibino, T.; Leroux, F.; Taviot-Guého, C. Layered Double Hydroxides. In *Developments in Clay Science*; Bergaya, F., Theng, B. K. G., Lagaly, G., Eds.; Elsevier: 2006; Vol. *1*, Chapter 13.1, pp 1021−1095.

(2) Miyata, S. Anion-Exchange Properties of Hydrotalcite-like Compounds. *Clay Clay Miner.* **1983**, *31*, 305−311.

(3) Meyn, M.; Beneke, K.; Lagaly, G. Anion-Exchange Reactions of Layered Double Hydroxides. *Inorg. Chem.* **1990**, *29*, 5201−5207.

(4) Rives, V. *Layered Double Hydroxides: Present and Future*; Nova Publishers: 2001.

(5) Cavani, F.; Trifiro, F.; Vaccari, A. Hydrotalcite-Type Anionic Clays: Preparation, Properties and Applications. *Catal. Today* **1991**, *11*, 173−301.

(6) Newman, S. P.; Jones, W. Synthesis, Characterization and Applications of Layered Double Hydroxides Containing Organic Guests. *New J. Chem.* **1998**, *22*, 105−115.

(7) Debecker, D. P.; Gaigneaux, E. M.; Busca, G. Exploring, Tuning, and Exploiting the Basicity of Hydrotalcites for Applications in Heterogeneous Catalysis. *Chem.—Eur. J.* **2009**, *15*, 3920−3935.

(8) Xu, Z. P.; Zhang, J.; Adebajo, M. O.; Zhang, H.; Zhou, C. Catalytic Applications of Layered Double Hydroxides and Derivatives. *Appl. Clay Sci.* **2011**, *53*, 139−150.

(9) Del Hoyo, C. Layered Double Hydroxides and Human Health: An Overview. *Appl. Clay Sci.* **2007**, *36*, 103−121.

(10) Mousty, C.; Leroux, F. LDHs as Electrode Materials for Electrochemical Detection and Energy Storage: Supercapacitor, Battery and (Bio)-Sensor. *Recent Pat. Nanotechnol.* **2012**, *6*, 174−192.

(11) Palmer, S. J.; Frost, R. L.; Nguyen, T. Hydrotalcites and Their Role in Coordination of Anions in Bayer Liquors: Anion Binding in Layered Double Hydroxides. *Coord. Chem. Rev.* **2009**, *253*, 250−267.

DOI: 10.1021/acs.jpcc.5b01578
J. Phys. Chem. C 2015, 119, 12356−12364

(12) Goh, K.-H.; Lim, T.-T.; Dong, Z. Application of Layered Double Hydroxides for Removal of Oxyanions: A Review. *Water Res.* **2008**, *42*, 1343−1368.
(13) Salak, A. N.; Tedim, J.; Kuznetsova, A. I.; Ribeiro, J. L.; Vieira, L. G.; Zheludkevich, M. L.; Ferreira, M. G. S. Comparative X-Ray Diffraction and Infrared Spectroscopy Study of Zn−Al Layered Double Hydroxides: Vanadate vs Nitrate. *Chem. Phys.* **2012**, *397*, 102−108.
(14) Zhang, M.; Reardon, E. J. Removal of B, Cr, Mo, and Se from Wastewater by Incorporation into Hydrocalumite and Ettringite. *Environ. Sci. Technol.* **2003**, *37*, 2947−2952.
(15) Paikaray, S.; Hendry, M. J. In Situ Incorporation of Arsenic, Molybdenum, and Selenium during Precipitation of Hydrotalcite-like Layered Double Hydroxides. *Appl. Clay Sci.* **2013**, *77*−*78*, 33−39.
(16) Paikaray, S.; Hendry, M. J.; Essilfie-Dughan, J. Controls on Arsenate, Molybdate, and Selenate Uptake by Hydrotalcite-like Layered Double Hydroxides. *Chem. Geol.* **2013**, *345*, 130−138.
(17) Smith, H. D.; Parkinson, G. M.; Hart, R. D. In Situ Absorption of Molybdate and Vanadate during Precipitation of Hydrotalcite from Sodium Aluminate Solutions. *J. Cryst. Growth* **2005**, *275*, e1665−e1671.
(18) Misono, M. Heterogeneous Catalysis by Heteropoly Compounds of Molybdenum and Tungsten. *Catal. Rev.* **1987**, *29*, 269−321.
(19) García-Gutiérrez, J. L.; Laredo, G. C.; García-Gutiérrez, P.; Jiménez-Cruz, F. Oxidative Desulfurization of Diesel Using Promising Heterogeneous Tungsten Catalysts and Hydrogen Peroxide. *Fuel* **2014**, *138*, 118−125.
(20) Chakravarty, R.; Shukla, R.; Tyagi, A. K.; Dash, A.; Venkatesh, M. Nanocrystalline Zirconia: A Novel Sorbent for the Preparation of 188W/188Re Generator. *Appl. Radiat. Isot.* **2010**, *68*, 229−238.
(21) Ikeda, S.; Neyts, J.; Yamamoto, N.; Murrer, B.; Theobald, B.; Bossard, G.; Henson, G.; Abrams, M.; Picker, D.; Declercq, E. In-Vitro Activity of a Novel Series of Polyoxosilicoviruses, Tungstates Against Human Myxoviruses, Herpesviruses and Retroviruses. *Antiviral Chem. Chemother.* **1993**, *4*, 253−262.
(22) Stephan, H.; Kubeil, M.; Emmerling, F.; Mueller, C. E. Polyoxometalates as Versatile Enzyme Inhibitors. *Eur. J. Inorg. Chem.* **2013**, No. 10−11, 1585−1594.
(23) Liu, J.; Wang, E. B.; Ji, L. N. The development of polyoxometalates as antivirus drugs. *Prog. Chem.* **2006**, *18*, 114−119.
(24) Witten, M. L.; Sheppard, P. R.; Witten, B. L. Tungsten Toxicity. *Chem.-Biol. Interact.* **2012**, *196*, 87−88.
(25) Clausen, J. L.; Bostick, B. C.; Bednar, A.; Sun, J.; Landis, J. D. *Tungsten Speciation in Firing Range Soils*; DTIC Document, 2011.
(26) Cruywagen, J. J. Protonation, Oligomerization, and Condensation Reactions of vanadate(V), molybdate(VI), and tungstate(VI). *Adv. Inorg. Chem.* **2000**, *49*, 127−182.
(27) Cruywagen, J. J.; van der Merwe, I. F. J. Tungsten(VI) Equilibria: A Potentiometric and Calorimetric Investigation. *J. Chem. Soc., Dalton Trans.* **1987**, No. 7, 1701−1705.
(28) Chen, Y.-G.; Gong, J.; Qu, L.-Y. Tungsten-183 Nuclear Magnetic Resonance Spectroscopy in the Study of Polyoxometalates. *Coord. Chem. Rev.* **2004**, *248*, 245−260.
(29) Himeno, S.; Takamoto, M.; Ueda, T. Formation of Alpha- and Beta-Keggin-Type [PW12O40](3-) Complexes in Aqueous Media. *Bull. Chem. Soc. Jpn.* **2005**, *78*, 1463−1468.
(30) Kwon, T.; Tsigdinos, G. A.; Pinnavaia, T. J. Pillaring of Layered Double Hydroxides (LDH's) by Polyoxometalate Anions. *J. Am. Chem. Soc.* **1988**, *110*, 3653−3654.
(31) Yun, S. K.; Pinnavaia, T. J. Layered Double Hydroxides Intercalated by Polyoxometalate Anions with Keggin (α-$H_2W_{12}O_{40}^{6-}$), Dawson (α-$P_2W_{18}O_{62}^{6-}$), and Finke ($Co_4(H_2O)_2(PW_9O_{34})_2^{10-}$) Structures. *Inorg. Chem.* **1996**, *35*, 6853−6860.
(32) Narita, E.; Kaviratna, P. D.; Pinnavaia, T. J. Direct Synthesis of a Polyoxometallate-Pillared Layered Double Hydroxide by Coprecipitation. *J. Chem. Soc., Chem. Commun.* **1993**, *No. 1*, 60−62.
(33) Weir, M. R.; Kydd, R. A. Synthesis of Heteropolyoxometalate-Pillared Mg/Al, Mg/Ga, and Zn/Al Layered Double Hydroxides via LDH−hydroxide Precursors. *Inorg. Chem.* **1998**, *37*, 5619−5624.
(34) Nijs, H.; Bock, M. D.; Vansant, E. F. Comparative Study of the Synthesis and Properties of Polyoxometalate Pillared Layered Double Hydroxides (POM-LDHs). *J. Porous Mater.* **1999**, *6*, 101−110.
(35) Gardner, E.; Pinnavaia, T. J. On the Nature of Selective Olefin Oxidation Catalysts Derived from Molybdate- and Tungstate-Intercalated Layered Double Hydroxides. *Appl. Catal., A* **1998**, *167*, 65−74.
(36) Del Arco, M.; Carriazo, D.; Gutiérrez, S.; Martín, C.; Rives, V. Synthesis and Characterization of New Mg_2Al-Paratungstate Layered Double Hydroxides. *Inorg. Chem.* **2004**, *43*, 375−384.
(37) Del Arco, M.; Carriazo, D.; Gutiérrez, S.; Martín, C.; Rives, V. An FT-IR Study of the Adsorption and Reactivity of Ethanol on Systems Derived from Mg2Al−W7O246− Layered Double Hydroxides. *Phys. Chem. Chem. Phys.* **2004**, *6*, 465−470.
(38) Guo, Y.; Li, D.; Hu, C.; Wang, Y.; Wang, E. Layered Double Hydroxides Pillared by Tungsten Polyoxometalates: Synthesis and Photocatalytic Activity. *Int. J. Inorg. Mater.* **2001**, *3*, 347−355.
(39) Maciuca, A.-L.; Dumitriu, E.; Fajula, F.; Hulea, V. Catalytic Oxidation Processes for Removing Dimethylsulfoxide from Wastewater. *Chemosphere* **2007**, *68*, 227−233.
(40) Davantès, A.; Lefèvre, G. In Situ Real Time Infrared Spectroscopy of Sorption of (Poly)molybdate Ions into Layered Double Hydroxides. *J. Phys. Chem. A* **2013**, *117*, 12922−12929.
(41) Ardau, C.; Frau, F.; Dore, E.; Lattanzi, P. Molybdate Sorption by Zn−Al Sulphate Layered Double Hydroxides. *Appl. Clay Sci.* **2012**, *65*−*66*, 128−133.
(42) Maestre, J. M.; Lopez, X.; Bo, C.; Poblet, J.-M.; Casañ-Pastor, N. Electronic and Magnetic Properties of A-Keggin Anions: A DFT Study of $[XM_{12}O_{40}]^{n-}$, (M = W, Mo; X = Al^{III}, Si^{IV}, P^{V}, Fe^{III}, Co^{II}, Co^{III}) and $[SiM_{11}VO_{40}]^{m-}$ (M = Mo and W). *J. Am. Chem. Soc.* **2001**, *123*, 3749−3758.
(43) López, X.; Maestre, J. M.; Bo, C.; Poblet, J.-M. Electronic Properties of Polyoxometalates: A DFT Study of A/β-$[XM_{12}O_{40}]^{n-}$ Relative Stability (M = W, Mo and X a Main Group Element). *J. Am. Chem. Soc.* **2001**, *123*, 9571−9576.
(44) Maestre, J. M.; Lopez, X.; Bo, C.; Poblet, J.-M.; Daul, C. A DFT Study of the Electronic Spectrum of the A-Keggin Anion $[Co^{II}W_{12}O_{40}]^{6-}$. *Inorg. Chem.* **2002**, *41*, 1883−1888.
(45) López, X.; Bo, C.; Poblet, J. M. Electronic Properties of Polyoxometalates: Electron and Proton Affinity of Mixed-Addenda Keggin and Wells−Dawson Anions. *J. Am. Chem. Soc.* **2002**, *124*, 12574−12582.
(46) Bagno, A.; Bonchio, M.; Sartorel, A.; Scorrano, G. Relativistic DFT Calculations of Polyoxotungstate 183W NMR Spectra: Insight into Their Solution Structure. *ChemPhysChem* **2003**, *4*, 517−519.
(47) López, X.; Poblet, J. M. DFT Study on the Five Isomers of $PW_{12}O_{40}^{3-}$: Relative Stabilization upon Reduction. *Inorg. Chem.* **2004**, *43*, 6863−6865.
(48) Alizadeh, M. H.; Salimi, A. R. Density Functional Theory and Hartree−Fock Studies: Geometry, Vibrational Frequencies and Electronic Properties of Anderson-Type Heteropolyanion, [XM6O24]n− (X=TeVI, IVII and M=Mo, W) and [SbVW6O24]7−. *Spectrochim. Acta, Part A* **2006**, *65*, 1104−1111.
(49) Ravelli, D.; Dondi, D.; Fagnoni, M.; Albini, A.; Bagno, A. Electronic and EPR Spectra of the Species Involved in [W10O32]4− Photocatalysis. A Relativistic DFT Investigation. *Phys. Chem. Chem. Phys.* **2013**, *15*, 2890−2896.
(50) Kresse, G.; Hafner, J. Ab Initio Molecular Dynamics for Liquid Metals. *Phys. Rev. B* **1993**, *47*, 558−561.
(51) Kresse, G.; Hafner, J. Norm-Conserving and Ultrasoft Pseudopotentials for First-Row and Transition Elements. *J. Phys.: Condens. Matter* **1994**, *6*, 8245.
(52) Perdew, J. P.; Burke, K.; Ernzerhof, M. Generalized Gradient Approximation Made Simple. *Phys. Rev. Lett.* **1996**, *77*, 3865−3868.
(53) Perdew, J. P.; Burke, K.; Ernzerhof, M. Generalized Gradient Approximation Made Simple [Phys. Rev. Lett. 77, 3865 (1996)]. *Phys. Rev. Lett.* **1997**, *78*, 1396−1396.
(54) Blöchl, P. E. Projector Augmented-Wave Method. *Phys. Rev. B* **1994**, *50*, 17953−17979.

DOI: 10.1021/acs.jpcc.5b01578
J. Phys. Chem. C 2015, 119, 12356−12364

(55) Kresse, G.; Joubert, D. From Ultrasoft Pseudopotentials to the Projector Augmented-Wave Method. *Phys. Rev. B* **1999**, *59*, 1758−1775.
(56) Evans, H. T.; Gatehouse, B. M.; Leverett, P. Crystal Structure of the heptamolybdate(VI)(paramolybdate) Ion, [Mo7O24]6−, in the Ammonium and Potassium Tetrahydrate Salts. *J. Chem. Soc., Dalton Trans.* **1975**, No. 6, 505−514.
(57) Maksimovskaya, R. I.; Burtseva, K. G. 17O and 183W NMR Studies of the Paratungstate Anions in Aqueous Solutions. *Polyhedron* **1985**, *4*, 1559−1562.
(58) Courcot, B.; Bridgeman, A. J. Structural and Vibrational Study of $[Mo_7O_{24}]^{6-}$ and $[W_7O_{24}]^{6-}$. *J. Phys. Chem. A* **2009**, *113*, 10540−10548.
(59) Giannozzi, P.; Baroni, S. Vibrational and Dielectric Properties of C60 from Density-functional Perturbation Theory. *J. Chem. Phys.* **1994**, *100*, 8537−8539.
(60) Esfarjani, K.; Hashi, Y.; Onoe, J.; Takeuchi, K.; Kawazoe, Y. Vibrational Modes and IR Analysis of Neutral Photopolymerized C60 Dimers. *Phys. Rev. B* **1998**, *57*, 223−229.
(61) Baroni, S.; de Gironcoli, S.; Dal Corso, A.; Giannozzi, P. Phonons and Related Crystal Properties from Density-Functional Perturbation Theory. *Rev. Mod. Phys.* **2001**, *73*, 515−562.
(62) Karhanek, D. Self-Assembled Monolayers Studied by Density-Functional Theory. PhD, uniwien: Wien, 2010.
(63) Karhánek, D.; Bučko, T.; Hafner, J. A Density-Functional Study of the Adsorption of Methane-Thiol on the (111) Surfaces of the Ni-Group Metals: II. Vibrational Spectroscopy. *J. Phys.: Condens. Matter* **2010**, *22*, 265006.
(64) Jolivet, J.-P. *De la solution a l'oxide*; InterÉditions/CNRS Éditions: Paris, 1994.
(65) Nakamoto, K. *Infrared and Raman Spectra of Inorganic and Coordination Compounds: Part A: Theory and Applications in Inorganic Chemistry*, 6th ed.; John Wiley & Sons: New Jersey, 2008.
(66) Allmann, R. Die Struktur Des Ammoniumparawolframates (NH4)10[H2W12O42].10H2O. *Acta Crystallogr. B* **1971**, *27*, 1393−1404.
(67) Thomas, G. S.; Kamath, P. V. Line Broadening in the PXRD Patterns of Layered Hydroxides: The Relative Effects of Crystallite Size and Structural Disorder. *J. Chem. Sci.* **2006**, *118*, 127−133.
(68) Thomas, G. S.; Rajamathi, M.; Kamath, P. V. DIFFaX Simulations of Polytypism and Disorder in Hydrotalcite. *Clay Clay Miner.* **2004**, *52*, 693−699.
(69) Drezdzon, M. A. Synthesis of Isopolymetalate-Pillared Hydrotalcite via Organic-Anion-Pillared Precursors. *Inorg. Chem.* **1988**, *27*, 4628−4632.
(70) Wang, J.; Tian, Y.; Wang, R. C.; Clearfield, A. Pillaring of Layered Double Hydroxides with Polyoxometalates in Aqueous Solution without Use of Preswelling Agents. *Chem. Mater.* **1992**, *4*, 1276−1282.
(71) Kwon, T.; Pinnavaia, T. J. Pillaring of a Layered Double Hydroxide by Polyoxometalates with Keggin-Ion Structures. *Chem. Mater.* **1989**, *1*, 381−383.
(72) George, B. L.; Aruldhas, G.; Botto, I. L. Vibrational Spectra of Sodium Paratungstate 26 Hydrate, Na10(H2W12O42)·26H2O. *J. Mater. Sci. Lett.* **1992**, *11*, 1421−1423.
(73) Lyhamn, L.; Haaland, A.; Seip, R.; Shen, Q.; Weidlein, J.; Spiridonov, V. P.; Strand, T. G. Multicomponent Polyanions. 33. Single Crystal Raman Spectra of Na6Mo7O24(H2O)14. *Acta Chem. Scand.* **1982**, *36a*, 595−603.

DOI: 10.1021/acs.jpcc.5b01578
J. Phys. Chem. C 2015, 119, 12356−12364